Electronic Supplementary Material (ESI) for New Journal of Chemistry.

Targeted Development of Sustainable Green Catalysts for Regioselective Acylation of Aromatic Ethers with Carboxylic Acids *via* Chlorosulfonic Acid Coated on Poly(guanidine-triazine-sulfonamide) Grafted γ-Fe_2O_3@quartz

Maryam Fereydooni, Sedigheh Alavinia, Ramin Ghorbani-Vaghei*

Department of Organic Chemistry, Faculty of Chemistry, Bu-Ali Sina University, Hamedan, 6517838683, Iran

*Corresponding author; E-mail: rgvaghei@yahoo.com & ghorbani@basu.ac.ir

Tel: +98(81)38380647

Characterization of γ-Fe_2O_3@quartz@PGTS-SO_3H nanocomposite

The FT-IR spectra of PGTSA, quartz, γ-Fe_2O_3@quartz, γ-Fe_2O_3@quartz@PGTSA, γ-Fe_2O_3@quartz@PGTS-SO_3H composite systems are shown in Fig. S1. In FT-IR spectrum of PGTSA, the broadband at 3200-3700 cm^{-1} indicates the presence of NH and NH_2. The vibration bands at 1338 and 1160 cm^{-1} (because of the O=S=O stretching) demonstrate the presence of sulfone bridges in the PGTSA. Also, absorption bands at 1664 and 1682 cm^{-1} indicate the presence of guanidine and melamine (Fig. S1a). In the quartz curve, the Si-O stretching vibration appeared at 1099 cm^{-1} (Fig. S1b). Fig. S1c illustrates the FT-IR spectrum of γ-Fe_2O_3@quartz. FT-IR analysis of γ-Fe_2O_3@quartz displayed a broad absorption band at 3000-3500 cm^{-1}, which is indexed to -SiOH groups' OH symmetric stretching vibrations. Two adsorption bands at 1087 cm^{-1} are indexed to the symmetric and asymmetric stretching vibrations of the Si-O-Si bond on the quartz surface. Also, the γ-Fe_2O_3 in the quartz structure can be detected through the band at 605 cm^{-1} (indexed to Fe–O bonds' stretching vibration). It is noteworthy that this band is covered by Si–O bonds' stretching vibrations. These results conform with those in the literature. After PGTSA immobilization on the γ-Fe_2O_3@quartz surface, the Fe-O bonds shifted to a higher wavelength (620 cm^{-1}) in the γ-Fe_2O_3@quartz@PGTSA spectrum. The broad peak at 3100-3400 cm^{-1} is attributed to the polymeric structure's NH and NH_2 groups (Fig. S1d). In the case of the γ-Fe_2O_3@ quartz @PGTSA-SO_3H catalyst, some additional peaks appeared at 629 $cm^{-1,}$ suggesting the successful anchoring of the chlorosulfonic acid to the γ-Fe_2O_3@quartz@PGTSA nanohybrid (Fig. S1e).

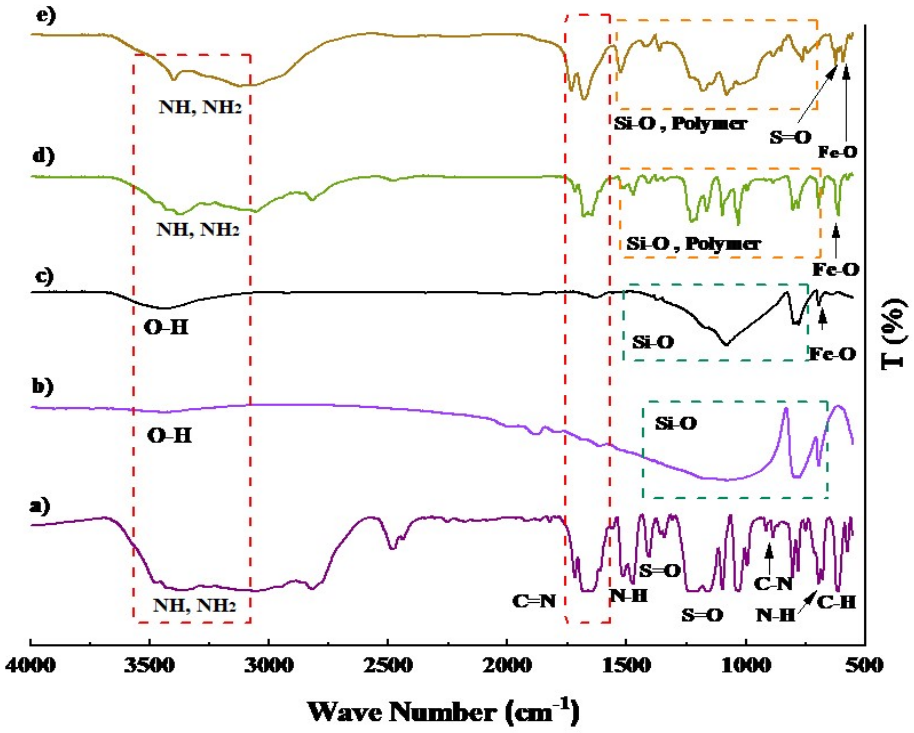

Fig. S1. FT-IR spectra of PGTSA (a), quartz (b), γ-Fe_2O_3@quartz (c), γ-Fe_2O_3@quartz@PGTSA (d), γ-Fe_2O_3@quartz@PGTS-SO_3H (e).

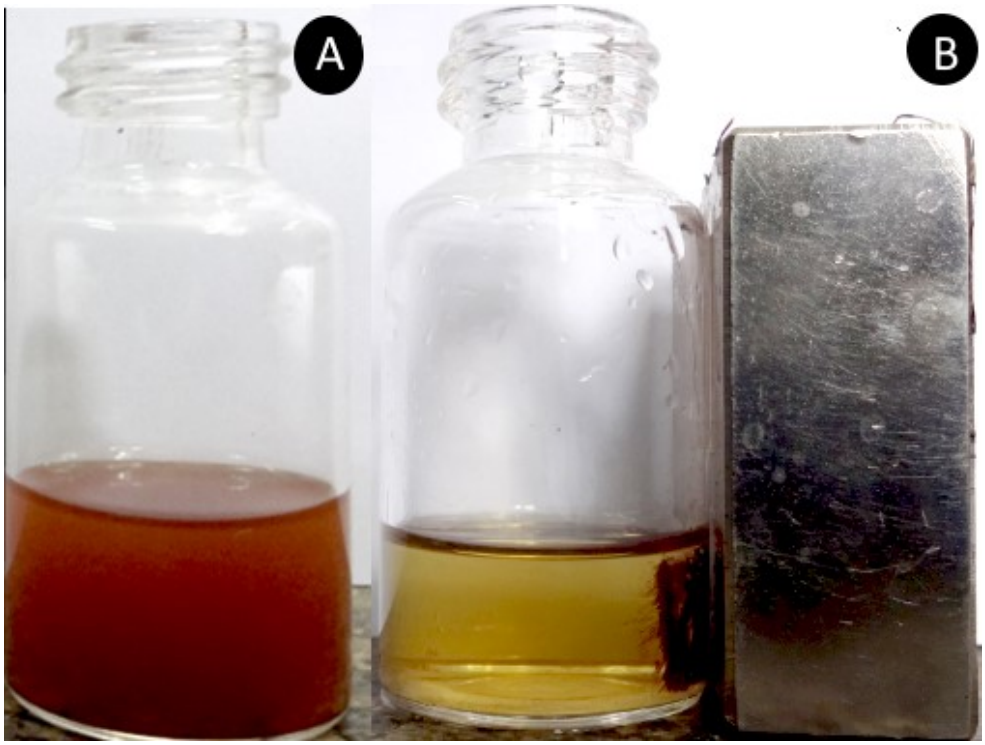

Fig. S2. Images of magnetic recovery A) before the reaction, B) after the rection.

^{1}H NMR (250 MHz, $CDCl_3$) δ 9.29 (s, 1H), 7.80 (d, *J* = 9.2 Hz, 1H), 7.62 (d, *J* = 8.0 Hz, 2H), 7.50 (s, 1H), 7.23 (d, *J* = 7.7 Hz, 2H), 3.84 (s, 3H), 3.45 (s, 3H). ^{13}C NMR (63 MHz, $CDCl_3$) δ 194.97, 156.21, 144.64, 139.03, 135.50, 129.94, 127.10, 126.44, 124.63, 122.98, 108.94, 56.06, 52.84, MS m/z (%): 287.

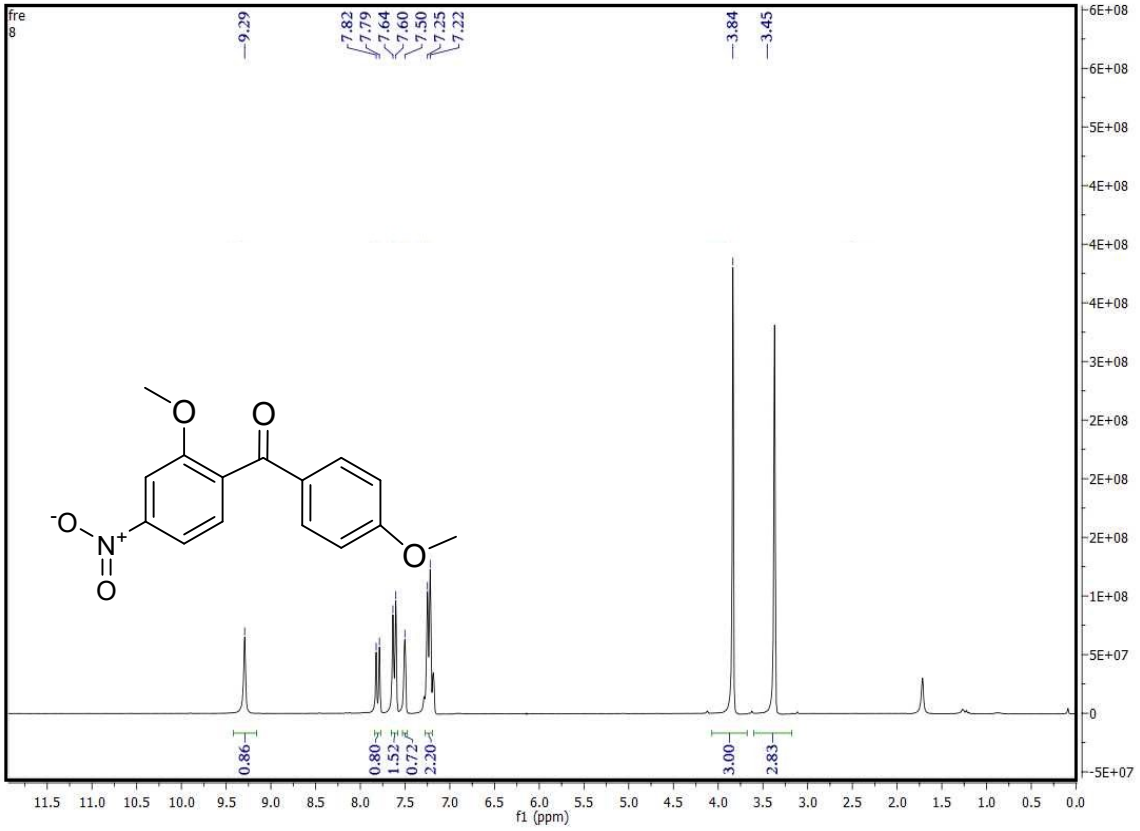

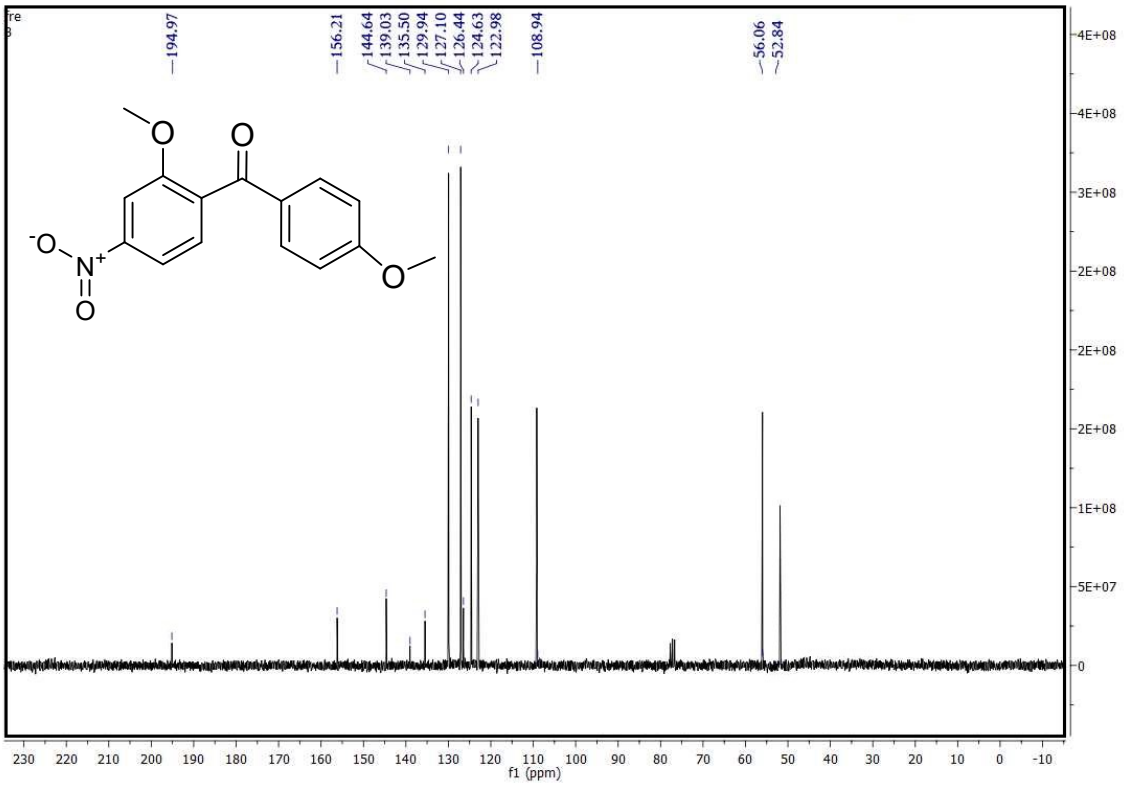
194.97
156.21
144.64
139.03
135.50
129.94
127.10
126.44
124.63
122.98
108.94
56.06
52.84
f1 (ppm)

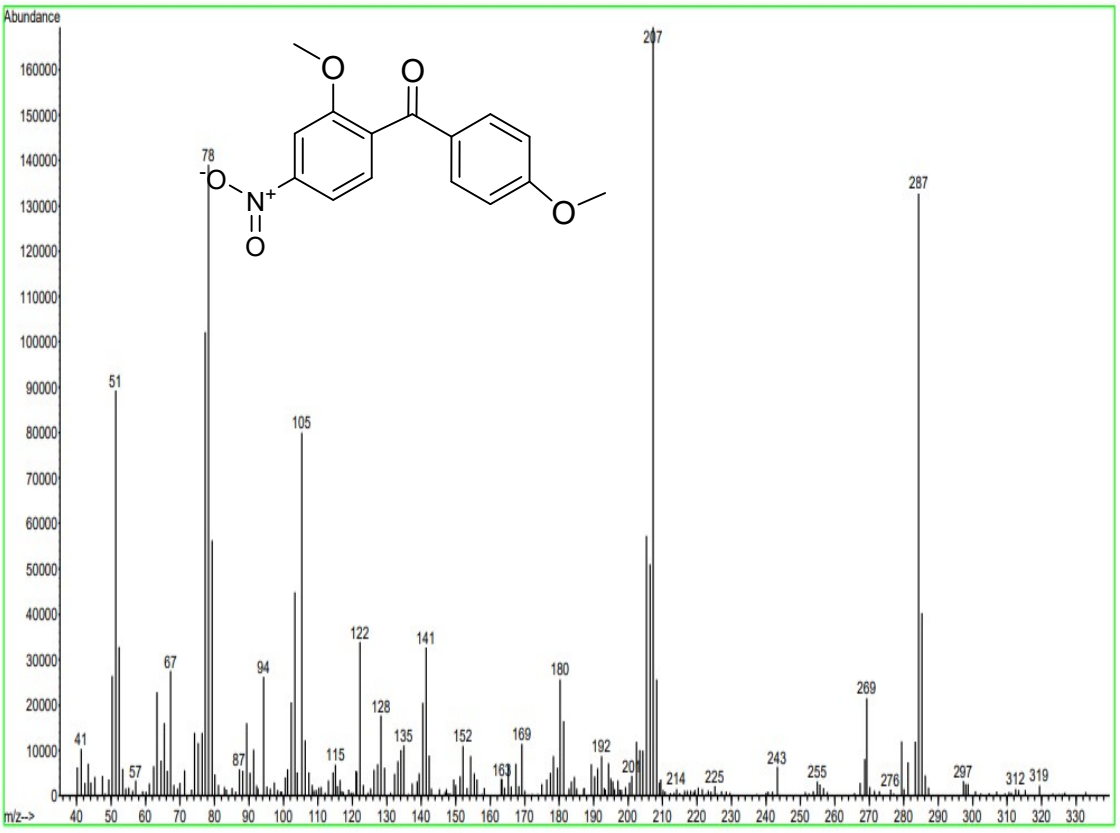
Abundance
m/z-->

^{1}H NMR (250 MHz, $CDCl_3$) δ 8.59 (s, 1H), 7.79 (s, 1H), 7.73 (d, *J* = 8.3 Hz, 2H), 7.40 (d, *J* = 8.7 Hz, 1H), 7.26 (d, *J* = 8.1 Hz, 2H), 3.88 (s, 3H). ^{13}C NMR (63 MHz, $CDCl_3$) δ 192.70, 150.32, 149.03, 144.08, 141.80, 136.19, 129.93, 126.97, 114.84, 113.57, 55.75. MS m/z (%): 290.

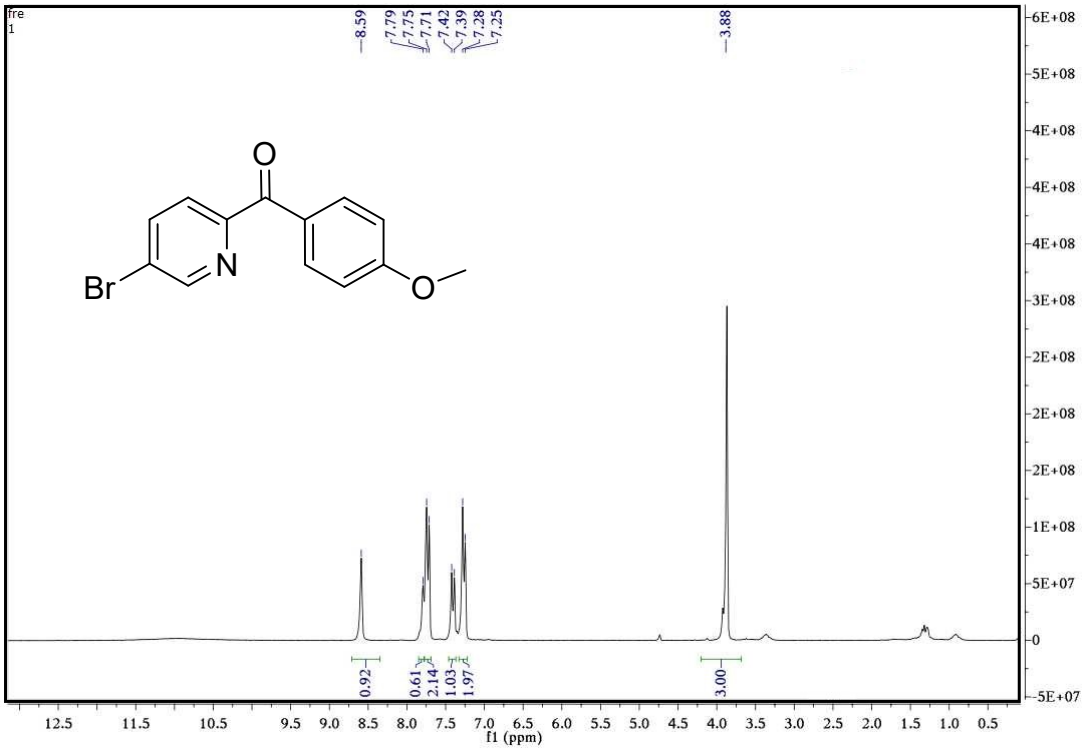

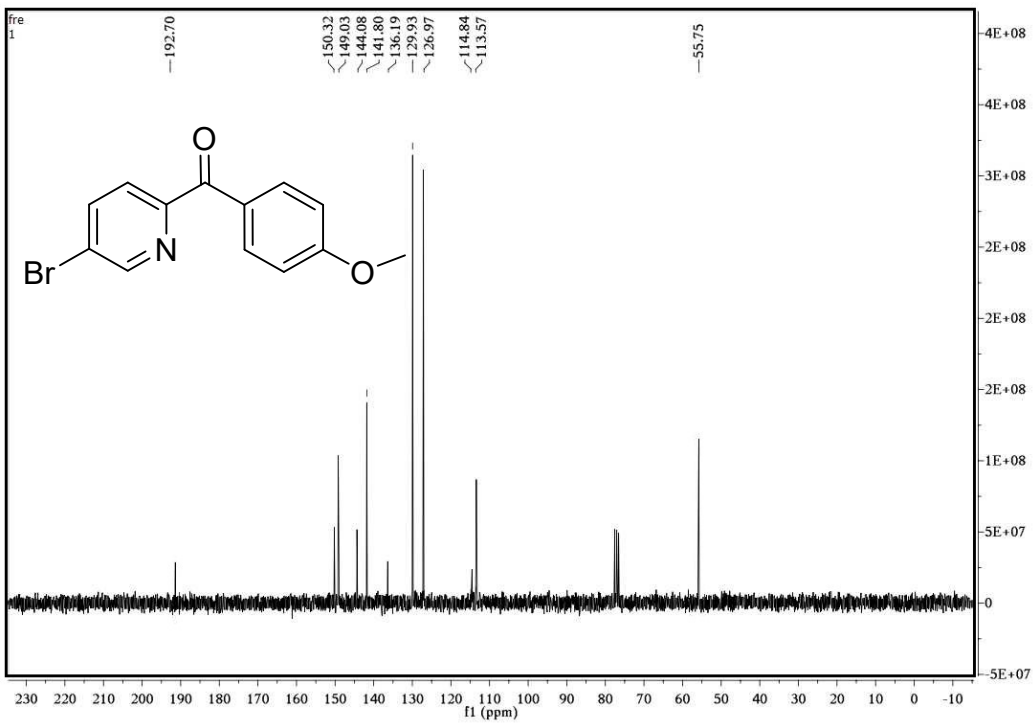

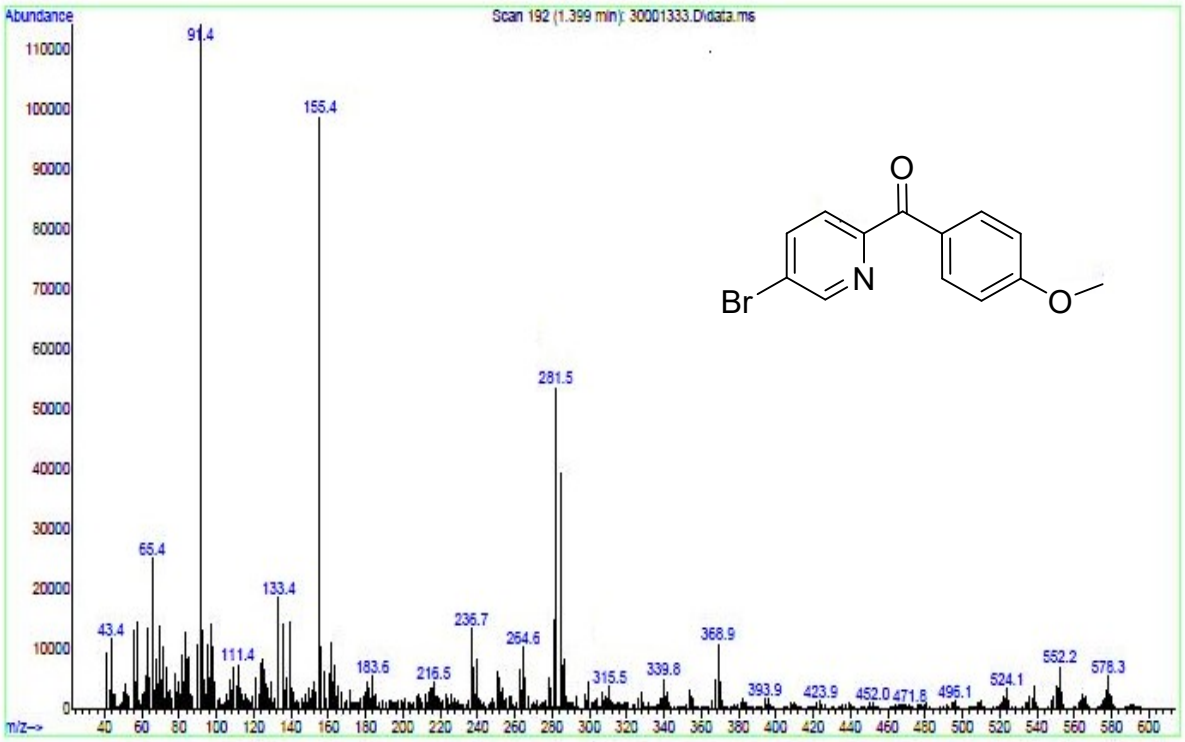

^{1}H NMR (250 MHz, $CDCl_3$) δ 7.71 (d, *J* = 7.8 Hz, 2H), 7.28 (d, *J* = 7.7 Hz, 2H), 7.20 (d, *J* = 8.6 Hz, 1H), 7.03 (d, *J* = 9.7 Hz, 2H), 3.70 (s, 3H). ^{13}C NMR (63 MHz, $CDCl_3$) δ 192.69, 144.36, 135.58, 134.85, 133.63, 130.02, 127.29, 126.04, 123.01, 121.79, 54.80. MS m/z (%): 280.

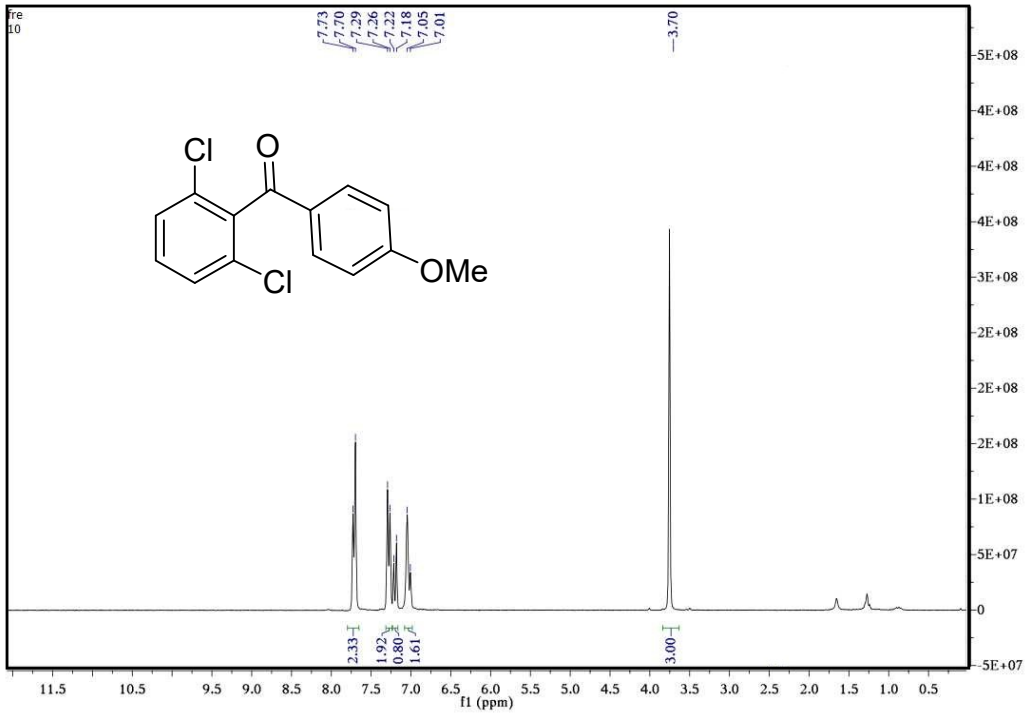
fre
10
7.73
7.70
7.29
7.26
7.22
7.18
7.05
7.01
3.70
Cl
O
Cl
OMe
2.33
1.92
0.80
1.61
3.00
f1 (ppm)

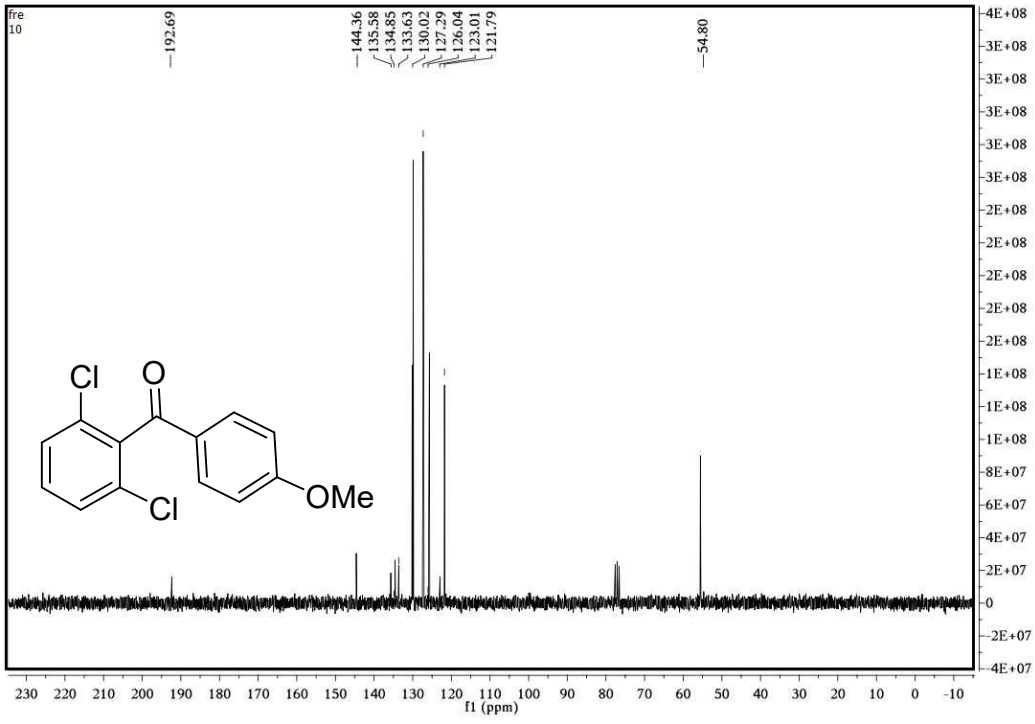
fre
10
192.69
144.36
135.58
134.85
133.63
130.02
127.29
126.04
123.01
121.79
54.80
Cl
O
Cl
OMe
f1 (ppm)

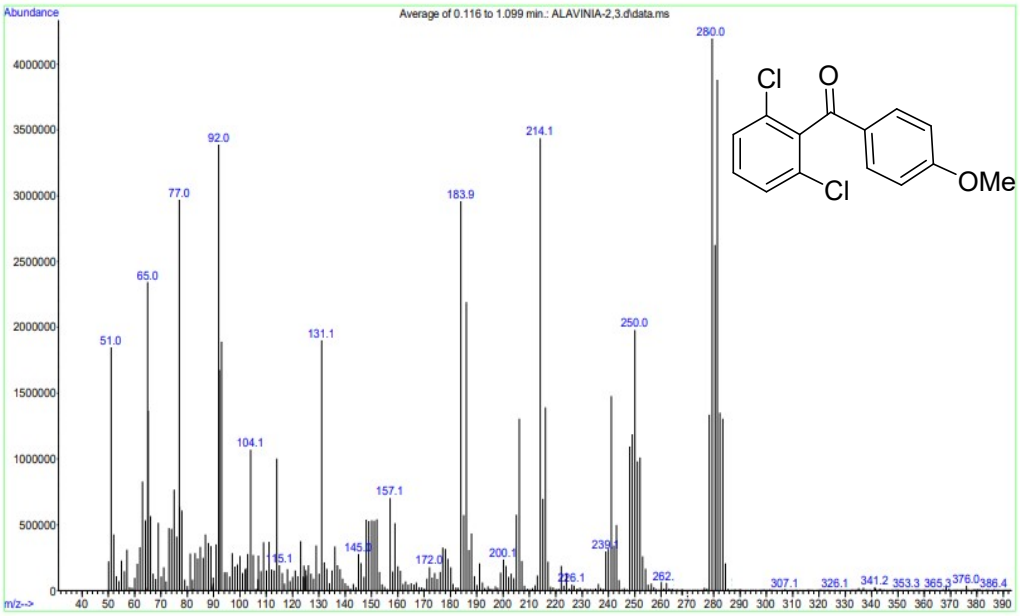

^{1}H NMR (250 MHz, DMSO-d_6) δ 8.12 (d, *J* = 8.9 Hz, 2H), 7.77 (d, *J* = 7.9 Hz, 2H), 7.39 (s, 1H), 7.35 (d, *J* = 4.8 Hz, 2H), 7.30 (s, 1H), 3.87 (s, 3H). ^{13}C NMR (63 MHz, DMSO) δ 197.27, 144.81, 144.52, 142.95, 136.64, 130.53, 127.24, 125.79, 118.35, 57.41. MS m/z (%): 257.

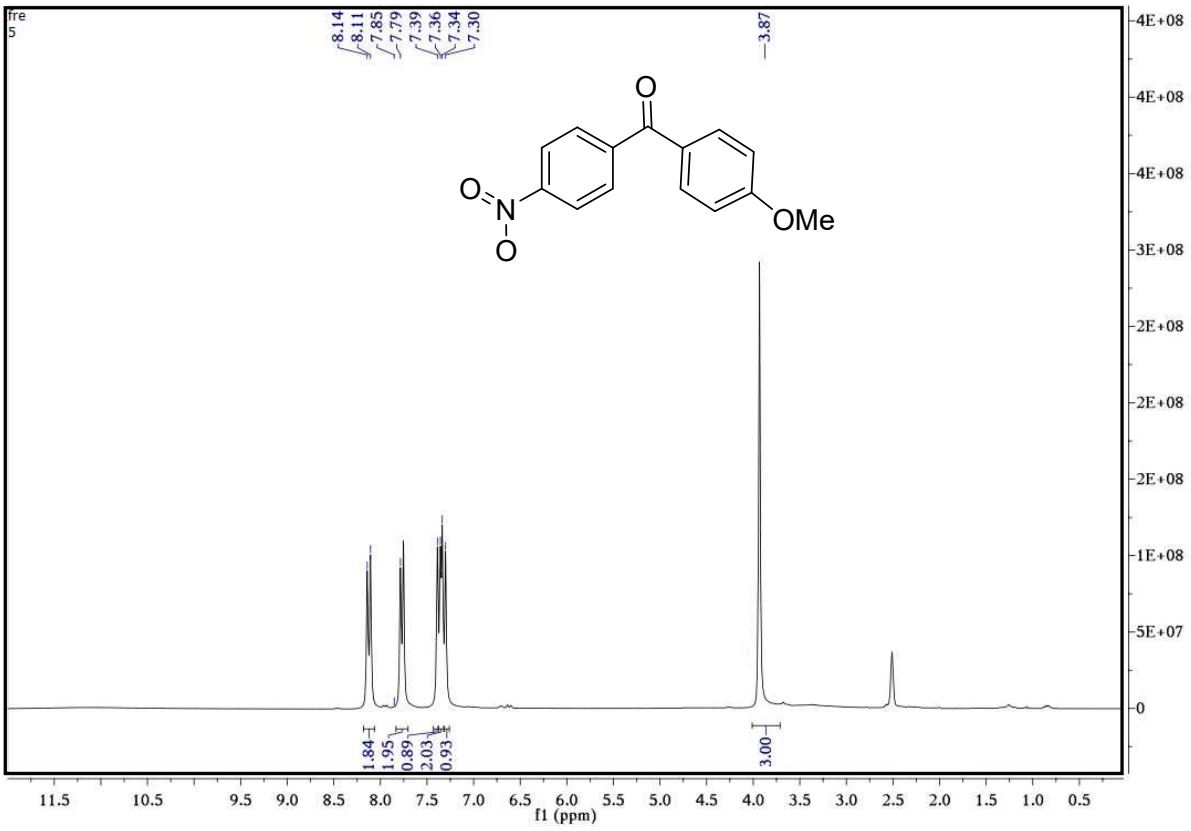

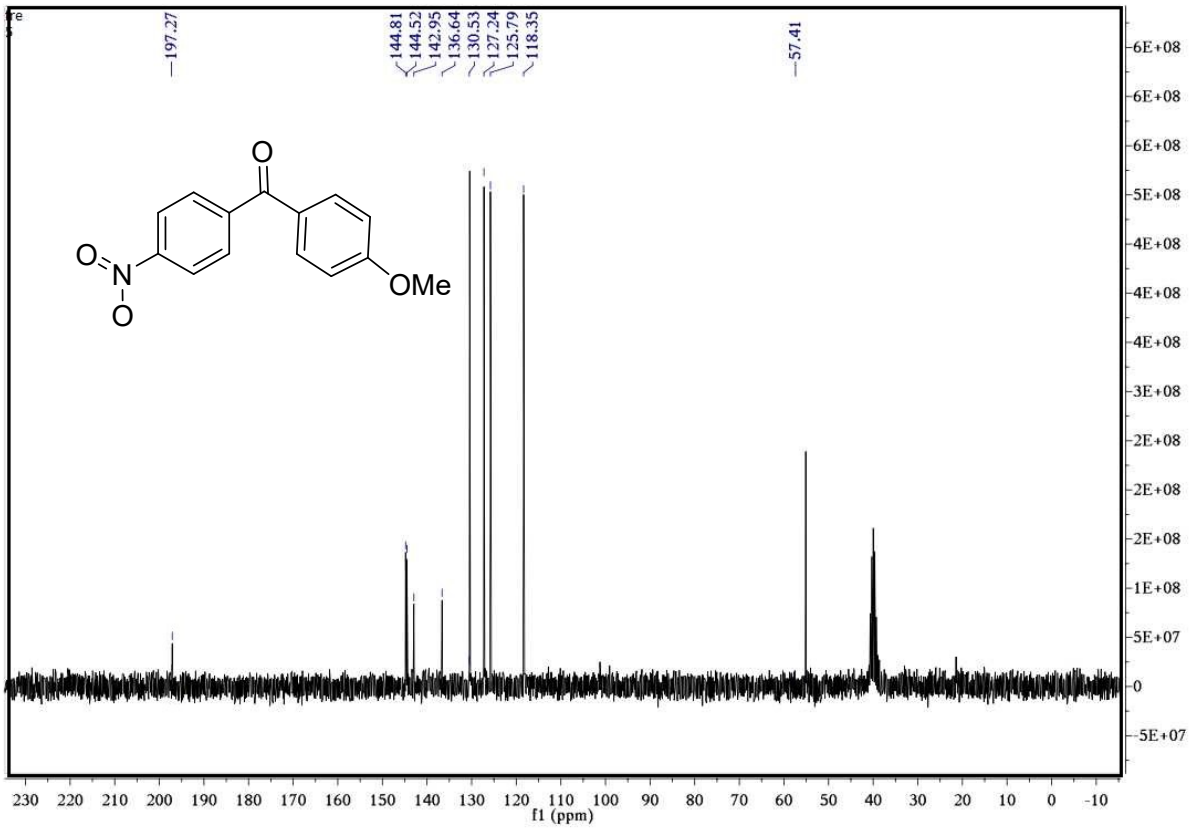
197.27
144.81
144.52
142.95
136.64
130.53
127.24
125.79
118.35
57.41
O
O
N
O
OMe
f1 (ppm)

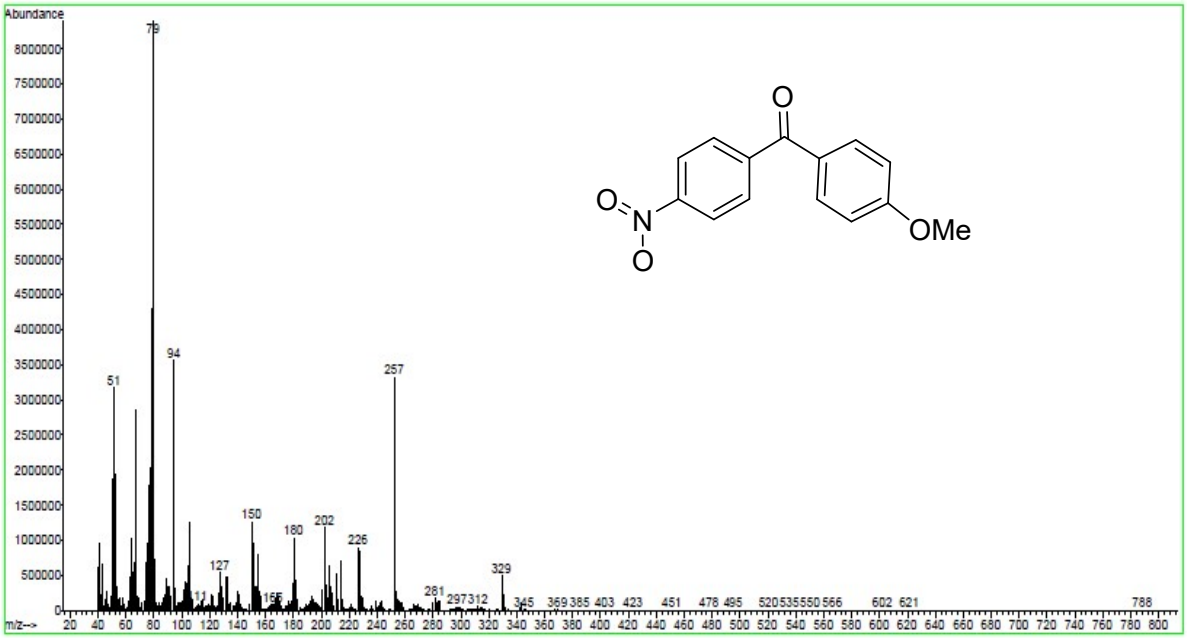
Abundance
m/z-->
O
O
N
O
OMe

^{1}H NMR (250 MHz, $CDCl_3$) δ 7.70 (d, *J* = 7.9 Hz, 2H), 7.45 (s, 1H), 7.27 (s, 1H), 7.23 (d, *J* = 5.0 Hz, 1H), 7.19 (s, 1H), 7.06 (d, *J* = 8.4 Hz, 2H), 3.61 (s, 3H). ^{13}C NMR (63 MHz, $CDCl_3$) δ 193.33, 153.31, 144.25, 135.63, 135.31, 130.72, 129.83, 129.39, 127.33, 122.75, 54.81. MS m/z (%): 291.

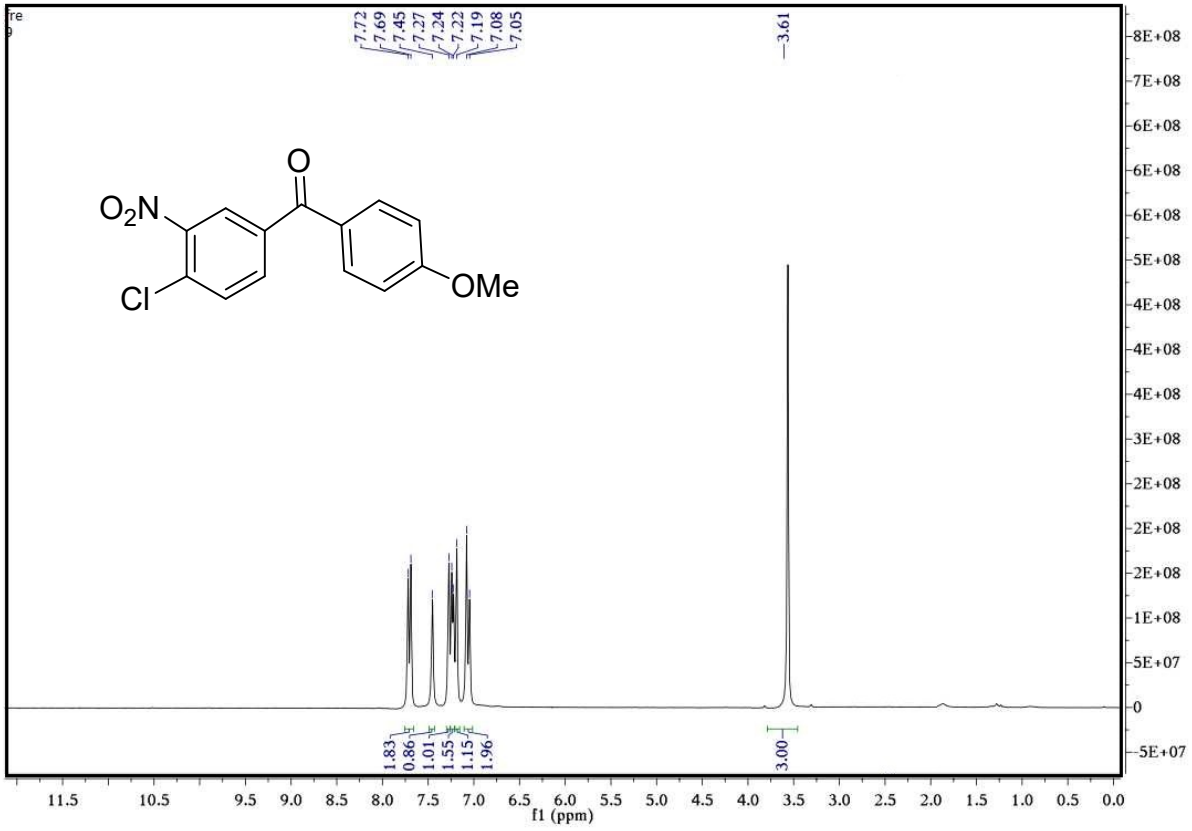

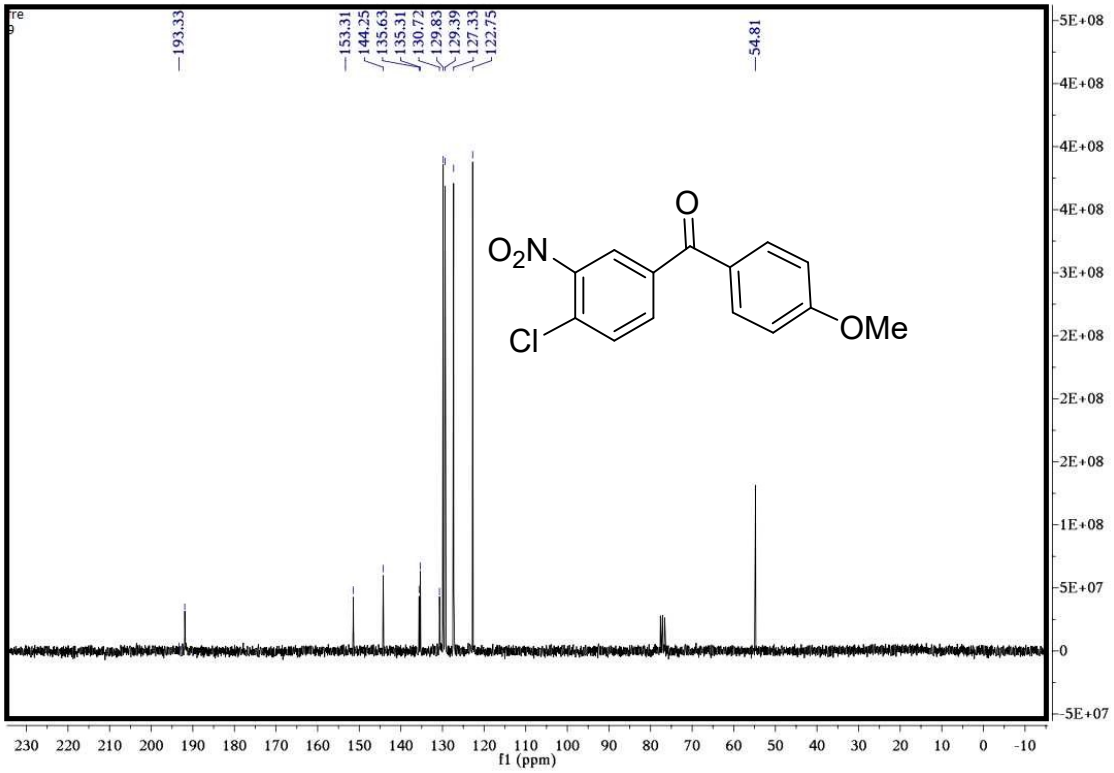
193.33
153.31
144.25
135.63
135.31
130.72
129.83
129.39
127.33
122.75
54.81
O
O2N
Cl
OMe
f1 (ppm)

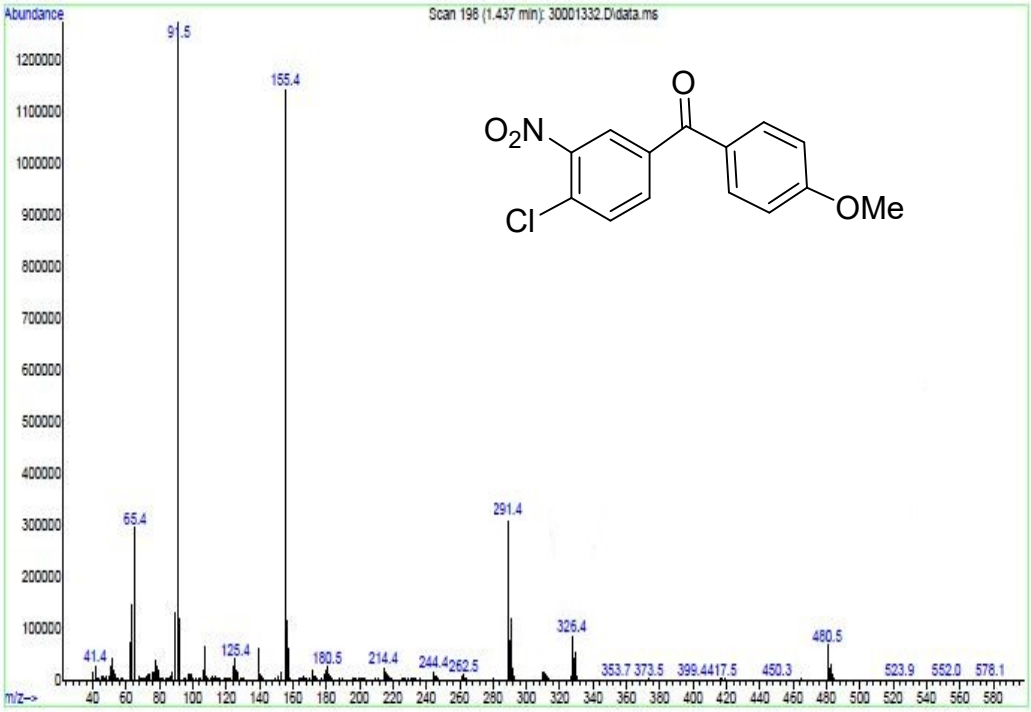
Abundance
Scan 198 (1.437 min): 30001332.D\data.ms
91.5
155.4
65.4
291.4
326.4
480.5
125.4
41.4
180.5
214.4
244.4
262.5
O
O2N
Cl
OMe
m/z-->

^{1}H NMR (250 MHz, $CDCl_3$) δ 8.69 (d, *J* = 4.8 Hz, 2H), 8.02 (d, *J* = 8.0 Hz, 2H), 7.31 (d, *J* = 8.2 Hz, 2H), 7.01 (t, *J* = 4.8 Hz, 1H), 3.45 (s, 3H). ^{13}C NMR (63 MHz, $CDCl_3$) δ 193.62, 158.49, 144.71, 136.51, 129.51, 128.63, 115.87, 55.44. MS m/z (%): 214.

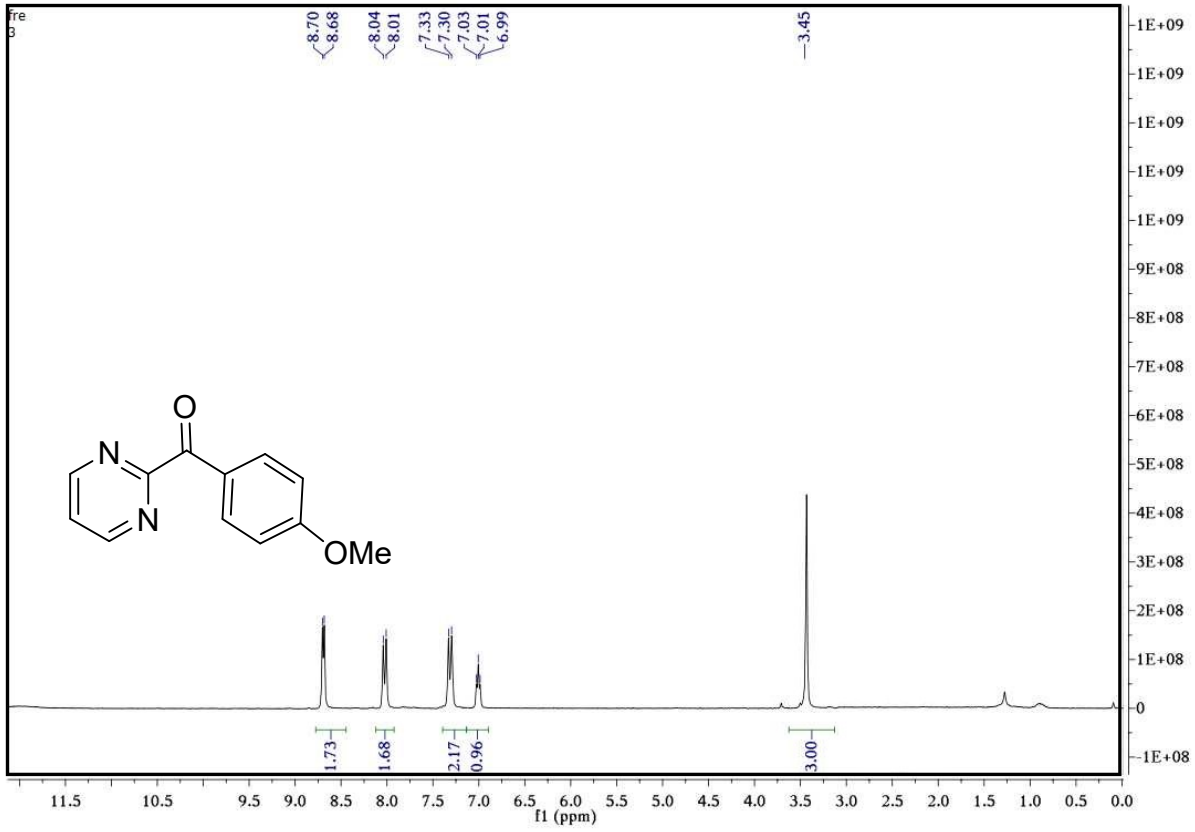

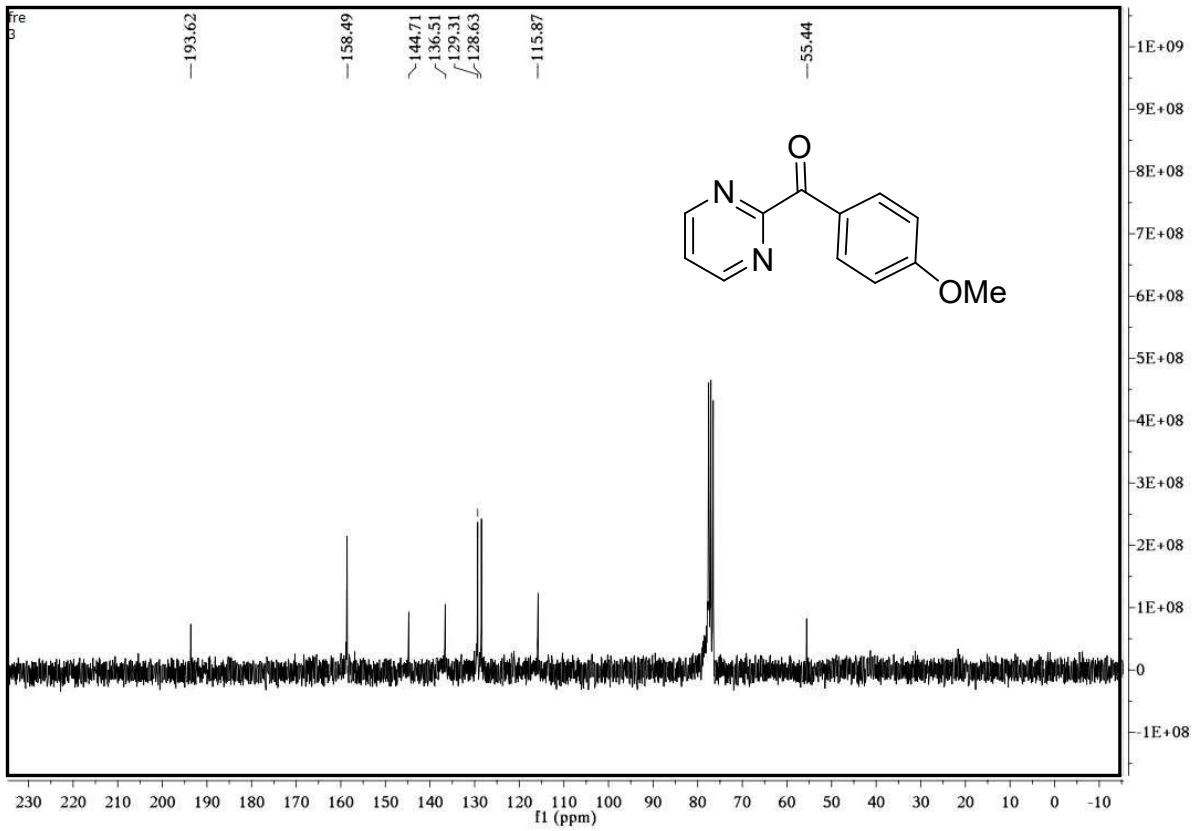

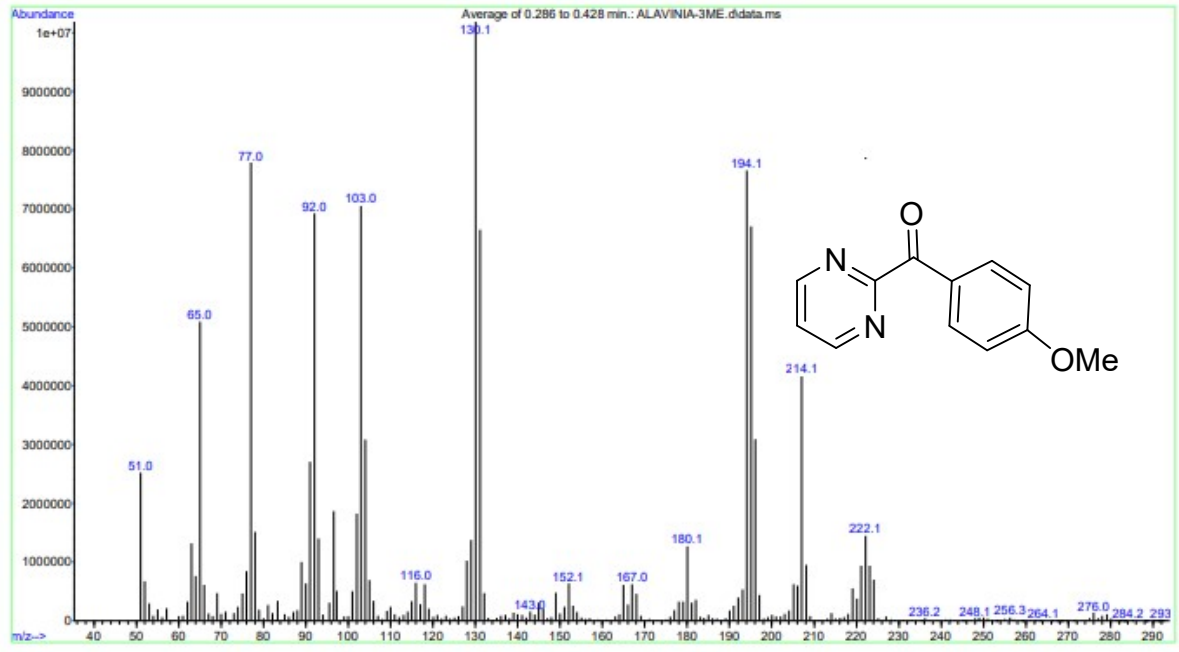

^{1}H NMR (250 MHz, $CDCl_3$) δ 7.95 (d, J = 8.9 Hz, 1H), 7.87 – 7.78 (m, 1H), 7.75 – 7.64 (m, 3H), 7.51 – 7.33 (m, 5H), 7.16 (d, J = 7.9 Hz, 2H), 3.65 (s, 3H). ^{13}C NMR (63 MHz, $CDCl_3$): δ: 57.40, 121.71, 122.62, 125.43, 126.28, 126.63, 127.12, 127.39, 128.36, 128.94, 129.58, 131.62, 134.26, 136.43, 143.78, 197.25. MS m/z (%): 261.

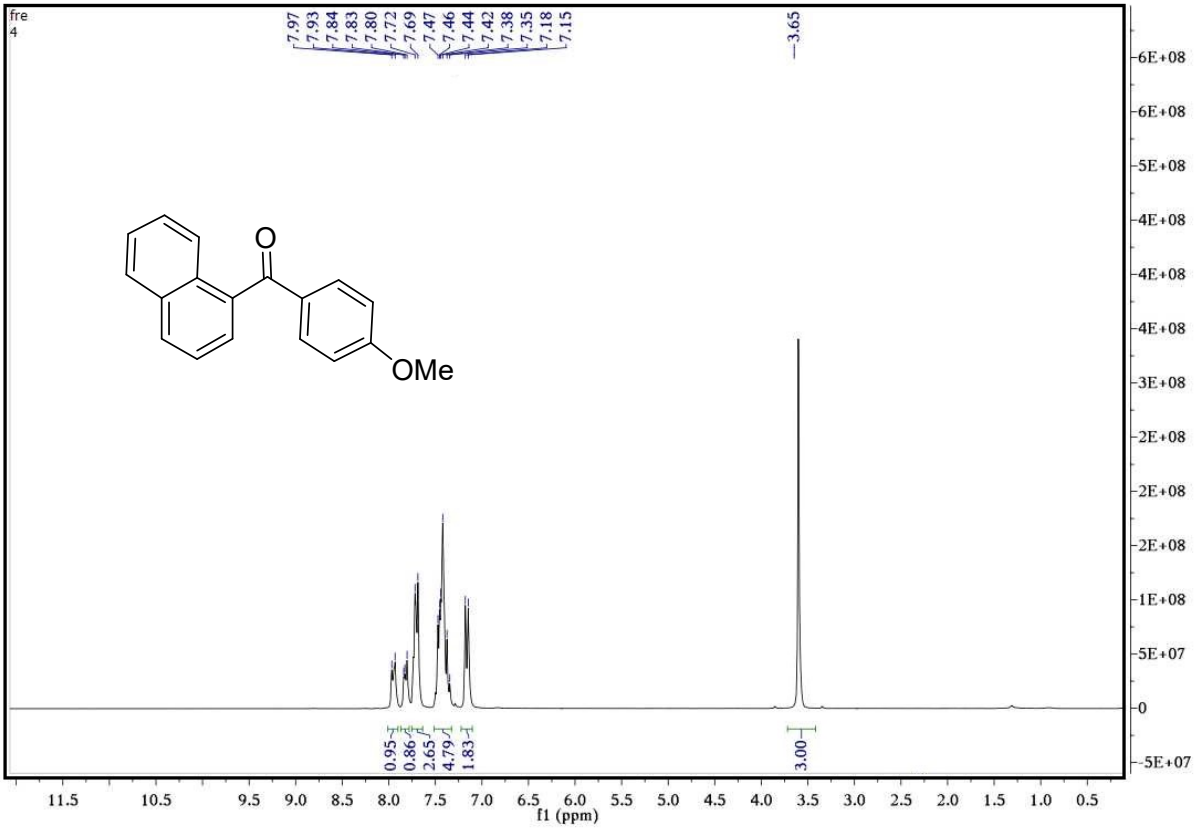
fre
4
7.97
7.93
7.84
7.83
7.80
7.72
7.69
7.47
7.46
7.44
7.42
7.38
7.35
7.18
7.15
3.65
O
OMe
0.95
0.86
2.65
4.79
1.83
3.00
f1 (ppm)

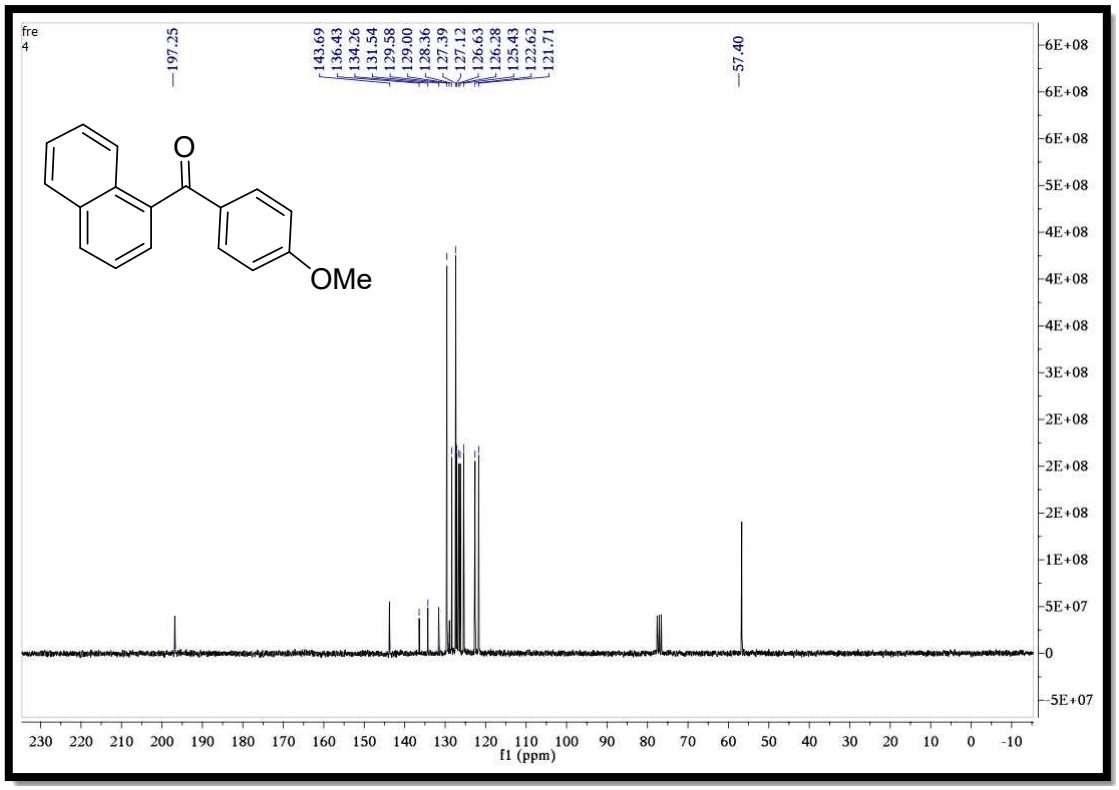
fre
4
197.25
143.69
136.43
134.26
131.54
129.58
129.00
128.36
127.39
127.12
126.63
126.28
125.43
122.62
121.71
57.40
O
OMe
f1 (ppm)

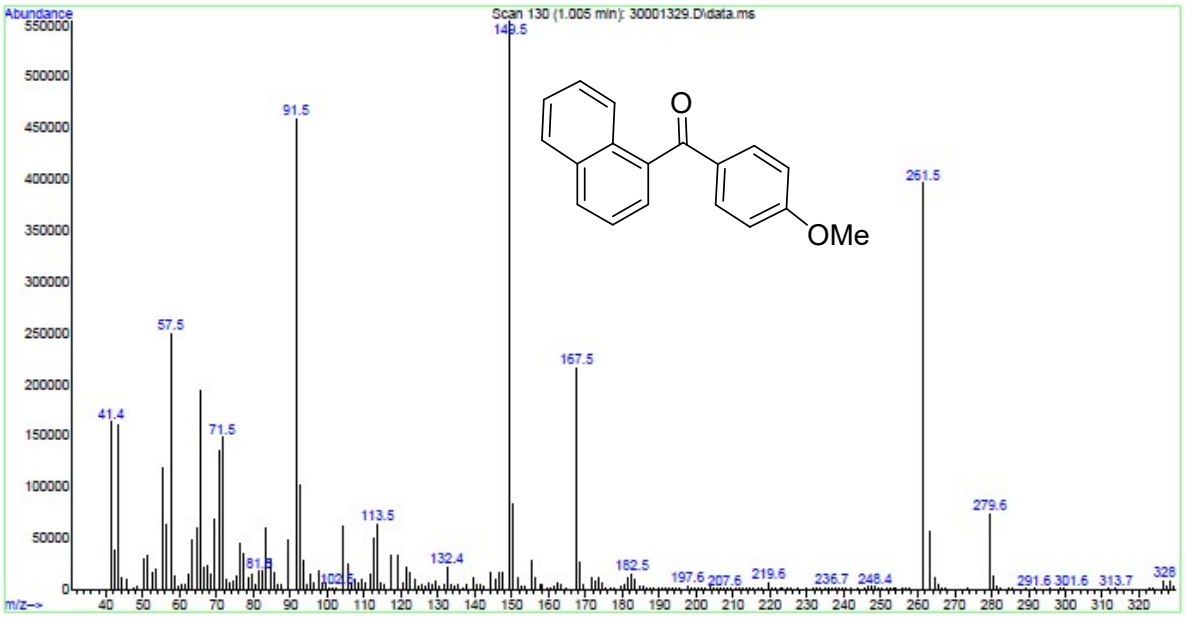

^{1}H NMR (250 MHz, DMSO-d_6) δ 8.04 (d, J = 7.9 Hz, 1H), 7.82 (d, J = 7.9 Hz, 1H), 7.37 (s, 3H), 7.39 (d, J = 8.2 Hz, 3H), 3.56 (s, 3H). ^{13}C NMR (63 MHz, DMSO-d_6) δ 191.36, 163.46, 158.43, 153.59, 147.41, 145.40, 143.43, 134.56, 131.63, 55.44. MS m/z (%): 213.

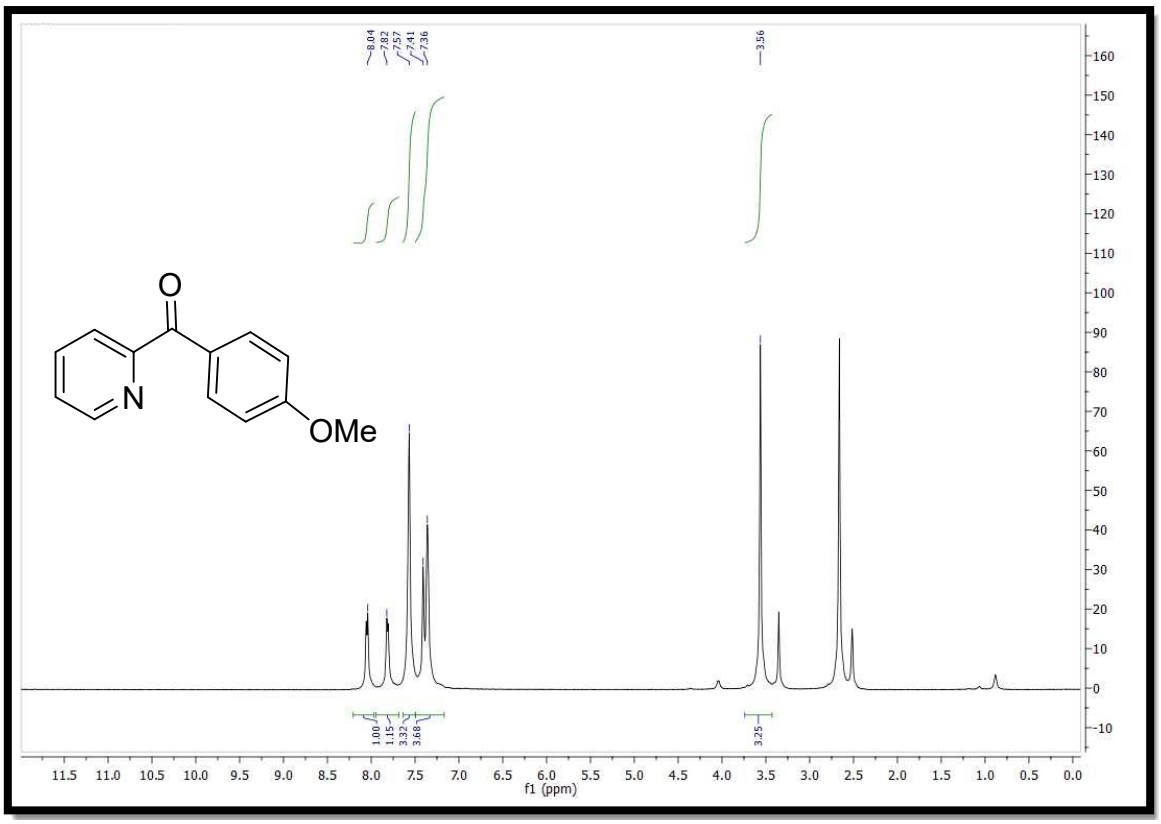

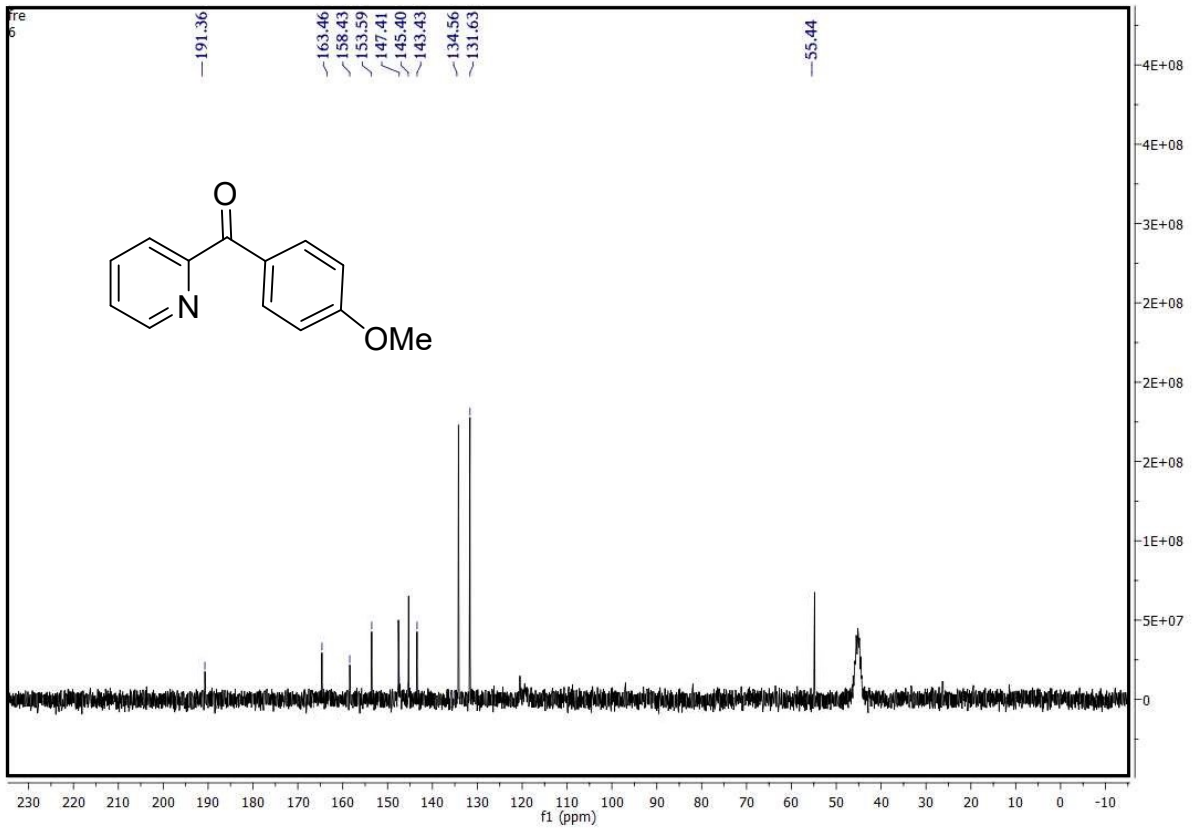

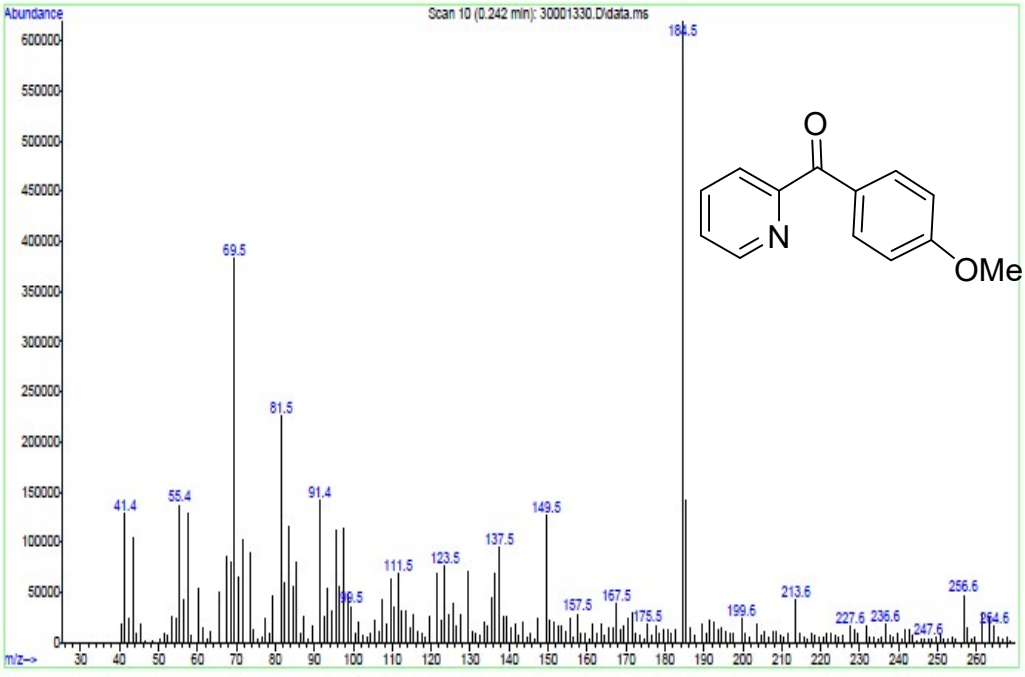

^{1}H NMR (250 MHz, $CDCl_3$) δ 7.76 (d, J = 8.1 Hz, 2H), 7.24 (d, J = 9.7 Hz, 2H), 5.41 (d, J = 7.0 Hz, 1H), 3.67 (s, 3H), 1.82 – 1.33 (m, 5H), 1.11 (d, J = 7.3 Hz, 5H)., ^{13}C NMR (63 MHz,

$CDCl_3$) δ 198.96, 142.98, 138.52, 129.57, 126.90, 58.55, 52.53, 33.66, 25.09, 24.59. MS m/z (%): 218.

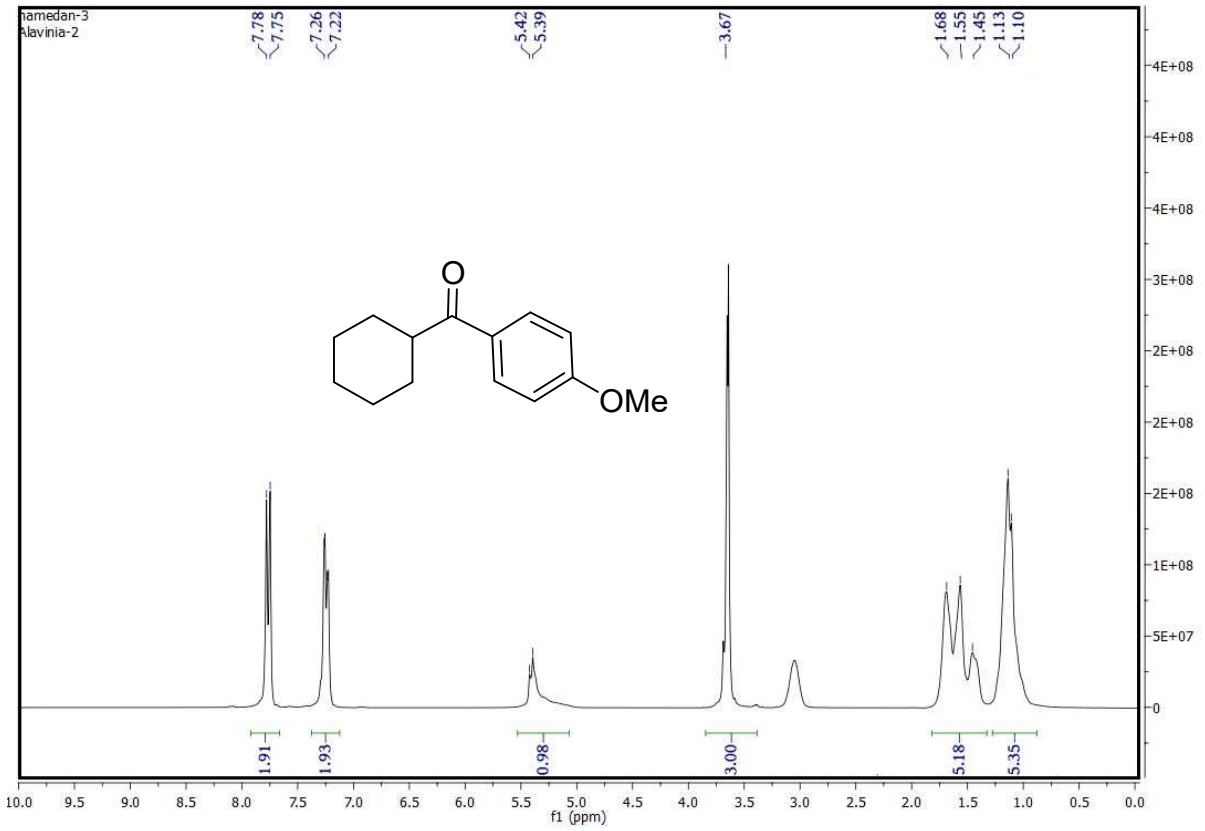

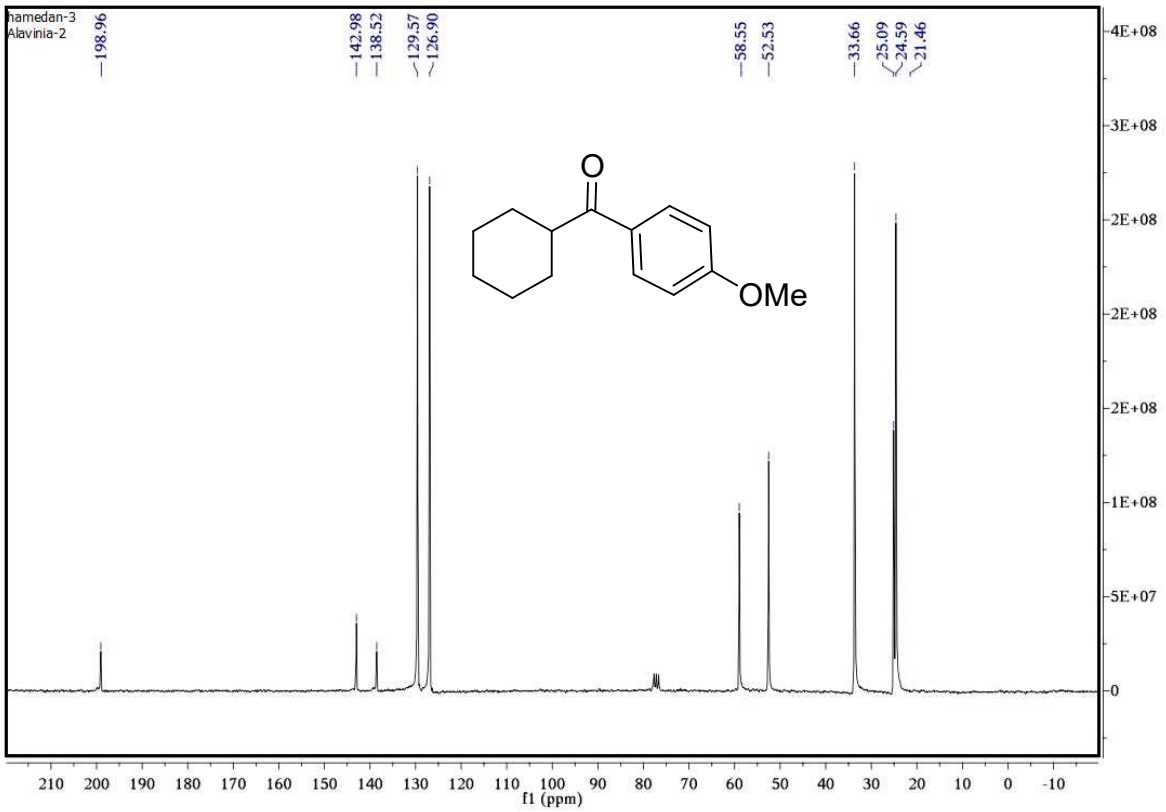

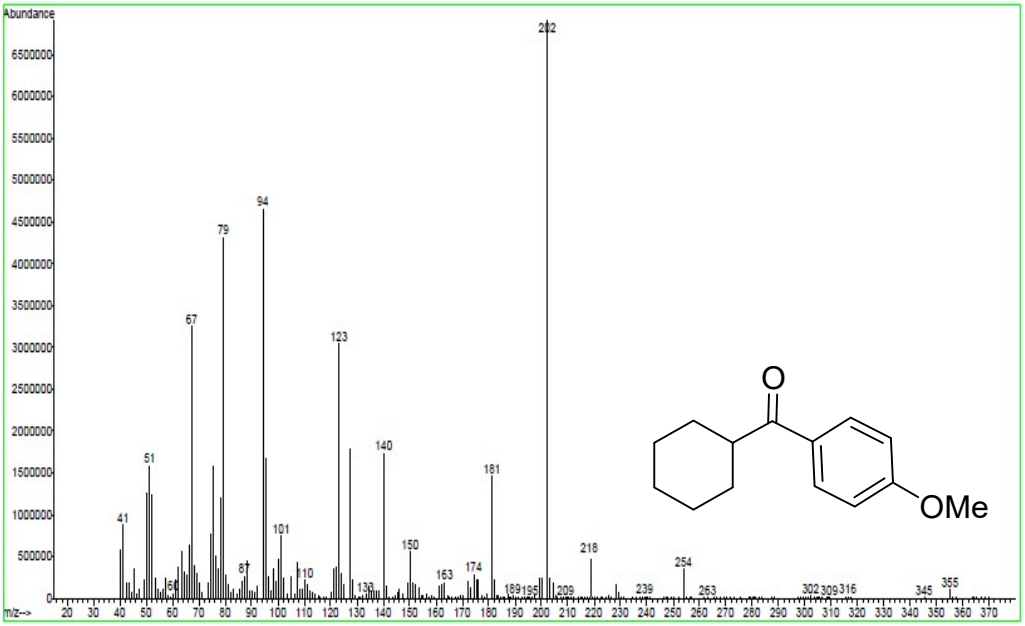

^{1}H NMR (250 MHz, $CDCl_3$) δ 7.78 (d, *J* = 6.6 Hz, 2H), 7.24 (d, *J* = 7.4 Hz, 2H), 5.39 (d, *J* = 11.2 Hz, 1H), 3.64 (s, 3H), 1.16 (s, 9H). ^{13}C NMR (63 MHz, $CDCl_3$) δ 196.50, 142.68, 140.63, 129.42, 126.92, 59.15, 54.38, 30.03. MS m//z (%): 192.8.

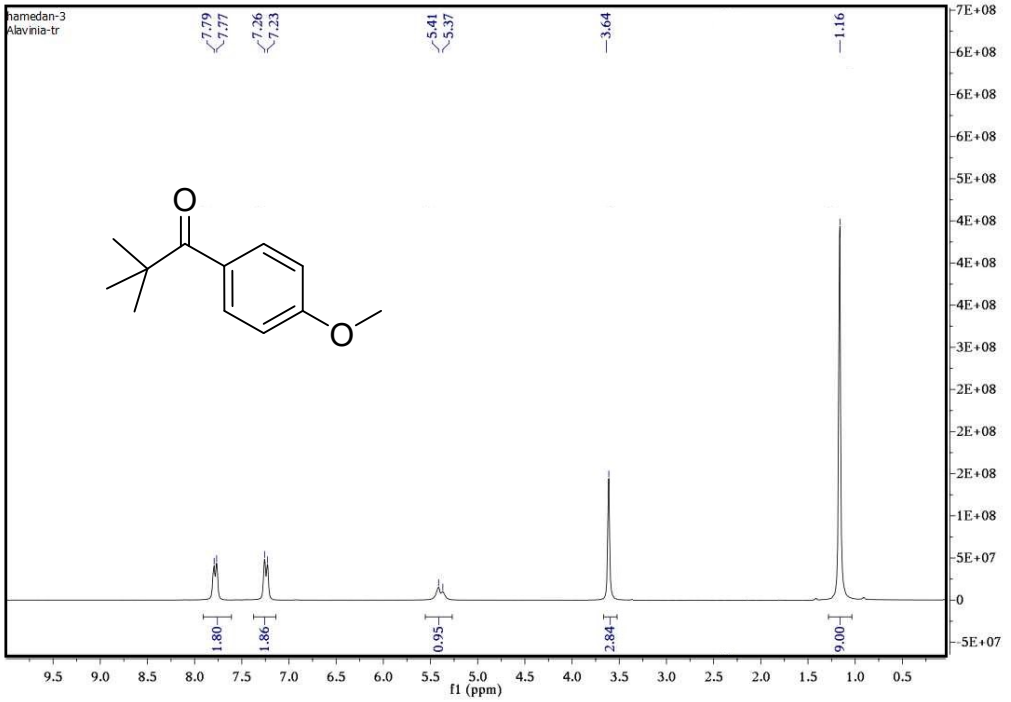
hamedan-3
Alavinia-tr
7.79
7.77
7.26
7.23
5.41
5.37
3.64
1.16
1.80
1.86
0.95
2.84
9.00
f1 (ppm)

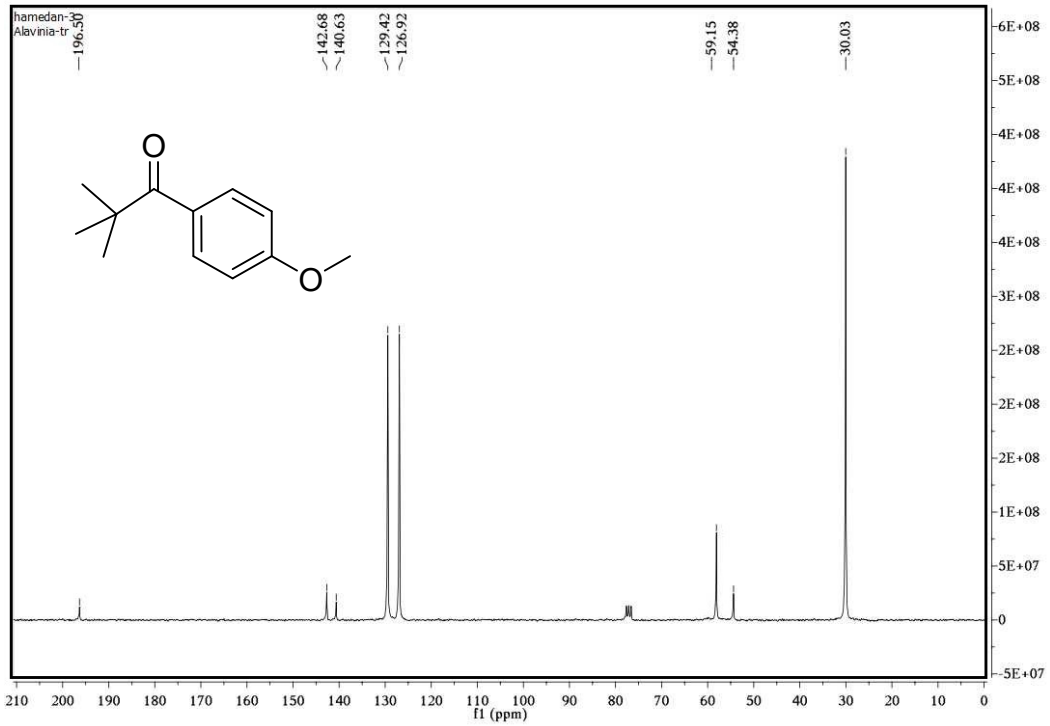
hamedan-3
Alavinia-tr
196.50
142.68
140.63
129.42
126.92
59.15
54.38
30.03
f1 (ppm)

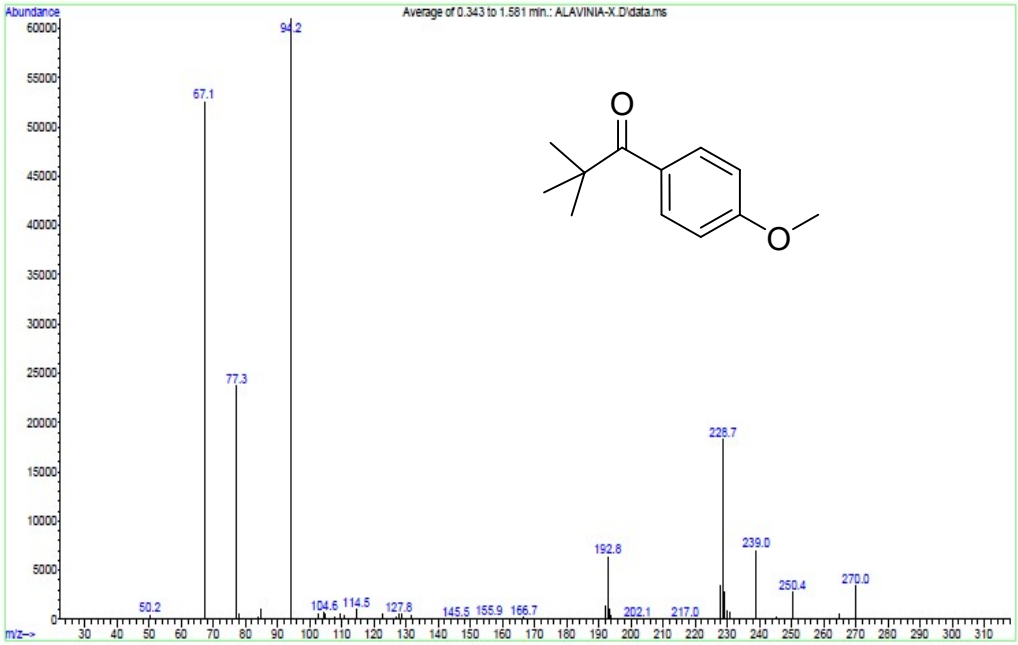
Abundance
Average of 0.343 to 1.581 min.: ALAVINIA-X.D\data.ms
94.2
67.1
77.3
228.7
192.8
239.0
250.4
270.0
50.2
104.6
114.5
127.8
145.5
155.9
166.7
202.1
217.0
m/z-->